



The effects of global awareness on the spreading of epidemics in multiplex networks

Haijuan Zang

College of Computer Engineering, Jiangsu University of Technology, 213001, Changzhou, China



HIGHLIGHTS

- The global awareness controlled spreading model is proposed to explore the coupled dynamical processes.
- We obtain the analytical results for the epidemic threshold by means of global microscopic Markov chain approach.
- Our model shows a strong restrain effects on epidemic spreading by comparison with other classical spreading models.

ARTICLE INFO

Article history:

Received 28 May 2017

Received in revised form 26 September 2017

Available online 20 November 2017

Keywords:

Complex network

Epidemic spreading

Global awareness

MMCA method

Multiplex network

ABSTRACT

It is increasingly recognized that understanding the complex interplay patterns between epidemic spreading and human behavioral is a key component of successful infection control efforts. In particular, individuals can obtain the information about epidemics and respond by altering their behaviors, which can affect the spreading dynamics as well. Besides, because the existence of herd-like behaviors, individuals are very easy to be influenced by the global awareness information. Here, in this paper, we propose a global awareness controlled spreading model (GACS) to explore the interplay between the coupled dynamical processes. Using the global microscopic Markov chain approach, we obtain the analytical results for the epidemic thresholds, which shows a high accuracy by comparison with lots of Monte Carlo simulations. Furthermore, considering other classical models used to describe the coupled dynamical processes, including the local awareness controlled contagion spreading (LACS) model, Susceptible–Infected–Susceptible–Unaware–Aware–Unaware (SIS–UAU) model and the single layer occasion, we make a detailed comparisons between the GACS with them. Although the comparisons and results depend on the parameters each model has, the GACS model always shows a strong restrain effects on epidemic spreading process. Our results give us a better understanding of the coupled dynamical processes and highlights the importance of considering the spreading of global awareness in the control of epidemics.

© 2017 Elsevier B.V. All rights reserved.

1. Introduction

The study of networks has experienced a burst of activity in the last two decades [1–5]. In the field of physics, most approaches to these problems are related to the theory of phase transition [6], statistical physics [7] and critical phenomenon [8–10]. Especially with the rapid development of Internet and social media, the study of diffusion processes has attracted more and more interests [11–13]. The use of network theory in epidemiological models provides a way to incorporate the individual-level heterogeneity necessary for the mechanistic understanding of the spread of infectious

E-mail address: zhjuan@jsut.edu.cn.

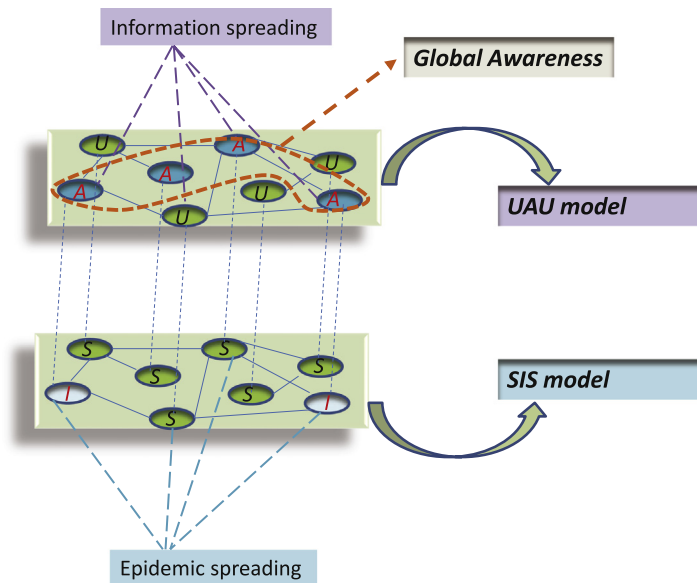


Fig. 1. The structure of GACS multiplex network model used in this paper. The upper layer corresponds to the network where the spreading of awareness happens; nodes on this layer have two kinds of states: unaware and aware. The lower layer represents the spreading of epidemics and the nodes also have two states: susceptible and infected. Only three states exist in the coupled dynamical processes, namely unaware and susceptible (US), aware and susceptible (AS), aware and infected (AI). Besides, the spreading models for the upper layer and lower layer are threshold model defined by the global awareness and contagion model, respectively.

disease [14]. And as a result, many interesting models have been proposed to help us to gain the details of these processes, such as the classical susceptible–infected–susceptible model (SIS) [15], susceptible–infected–recovery model (SIR) [16] and so on [17,18]. Different models correspond to diverse realistic scenarios and they may focus on various factors which can affect epidemic spreading, e.g., the structure of networks [19], the frequency of contacts among individuals [20], the heterogeneity of participants [21], the transmission capacity of community structure [22,23], etc.

Besides, with the development of technology, the information caused by epidemics can quickly diffuse through various channels, such as online social networks, the word of mouth, news media and so on. And the interplay between awareness and disease spreading processes is also a key issue in studying epidemics [24]. Therefore, to understand how information diffusion can mitigate epidemic outbreaks, and more broadly, the asymmetric interacting spreading dynamics has led to a new direction of research in complex network science [22]. Since the diffusion pathways of the two dynamical processes are quite different, it is difficult for us to study the coupled processes on the single layer network which consists of a single type of entity, with different entities connected to each other via a single type of connection. Consequently, as a natural way to describe the interrelated complex connections among individuals, multiplex network is gaining more and more attention owing to the reason that it can overcome the drawbacks of simplex network in which individuals interact only through one network [25–29]. It has also now been recognized that the study of multiplex networks is fundamental for enhancing the understanding of dynamical processes on networked systems [30]. Under the framework of multiplex network, there has been growing interest in exploring the interplay between epidemic spreading with human response, since it is natural for people to take measures when they become aware of epidemics [31–37]. A lot of works have studied the problem through different views, such as, Granell et al. proposed a SIS–UAU model by considering the information spreading process as a SIS model and discovered the emergence of a metacritical point where the diffusion of awareness is able to control the onset of epidemics [38]. Whereas Guo et al. replaced the SIS model by a threshold model and found a two-stage effect on epidemic threshold [39]. Wang et al. studied the asymmetrically interacting spreading dynamics based on a two SIR processes coupled model in multiplex networks, and found that the outbreak of disease can lead to the propagation of information [40]. Liu et al. studied the impact of non-Markovian vaccination adoption behavior on the epidemic dynamics and the control effects [22].

Actually, considering the spring up of various social media platforms, including Facebook, Twitter and Weibo, individuals are becoming more and more impressionable to the social focus [41,42]. That is to say, apart from the local awareness spreading, individuals are also very easy to be influenced by the global awareness information. The global awareness somehow represents the trends of the whole population, which can make it easy for individuals to adopt the awareness information. Hence, in this paper, we propose a global awareness controlled spreading model (GACS) to study the interplay between global awareness spreading and epidemic spreading. We have also extended the microscopic Markov chain approach (MMCA) to derive the epidemic threshold of the model analytically. And the method shows high accuracy for

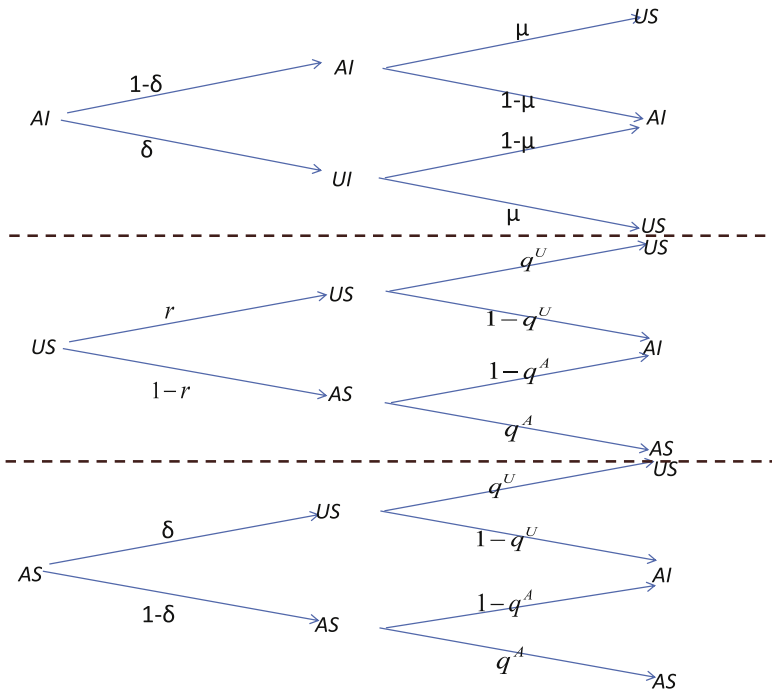


Fig. 2. The probability trees for the transitions of states. The states include AI (aware and infected), US (unaware and susceptible), AS (aware and susceptible). The meanings of parameters are as follows: μ represents transition probability from infected to susceptible, δ represents transition probability from aware to unaware, q^A (q^U) represents transition probability for individual not being infected by neighbors if it is aware (unaware), r represents probability for individual not changing from unaware to aware. The coupled dynamical processes take place consecutive as time goes by.

the prediction of the epidemic threshold, crosschecked by extensive Monte Carlo (MC) simulations. Furthermore, taking other classical models used to describe the coupled dynamical processes into consideration, including the local awareness controlled contagion spreading model (LACS), SIS–UAU model and the single layer occasion, we make a detailed comparisons between the GACS with them. Different with the LACS model, in the GACS model, there is no two-stage effect. And the suppression effects of the GACS is not always stronger or weaker than that of the LACS model, this depends on the local awareness threshold α . Moreover, compared with the SIS–UAU model, although it is easier for the outbreak of epidemics, the final epidemic size is always smaller. It is also very interesting that after we take account of the global awareness, compared with single layer occasion, the epidemic threshold increases and the final epidemic size also becomes smaller, which reveals the strong restrain effects of the GACS model.

2. The global awareness controlled contagion spreading model

Let us start from the definition of our GACS model. We build a two-layer network to illustrate it, as shown in Fig. 1. The upper layer represents the awareness spreading layer, while the lower layer is the contagion spreading layer. On the upper layer, if one individual is aware of epidemics, its state is Aware (A), otherwise its state is Unaware (U). The lower layer corresponds to the individual’s physical states of epidemics, if an individual is infected, its state is Infected (I), else its state is Susceptible (S). For the sake of simplicity, we assume that the multiplex network is unweighted and undirected. The interconnections between two layers are responsible for the coupled dynamical processes of the spreading of epidemics and awareness. It is worth noting that each individual can only have three kinds of states: unaware and susceptible (US), aware and infected (AI), aware and susceptible (AS), just as shown in Fig. 1.

As for the awareness spreading process on the upper awareness layer, the evolution of the states is defined as follow: the unaware individual can become aware with the probability which equals to the percentage of aware individuals of the whole population or unaware individuals are infected already. This means that the more aware individuals exist, the more easily unaware individuals become aware. Besides, the aware individual can also be unaware if it forgets the awareness (with a probability δ). Under the assumption of the SIS model for the spreading of epidemic, a susceptible individual can be infected by an infected neighbor with the probability β and infected ones can recover to be susceptible with probability μ at the same time. Note that the infectivity β of an individual will be reduced by a factor if it is aware, which makes us use β^U and β^A to represent the infection rates without and with awareness, respectively. Here we assume $\beta^A = 0$ and it

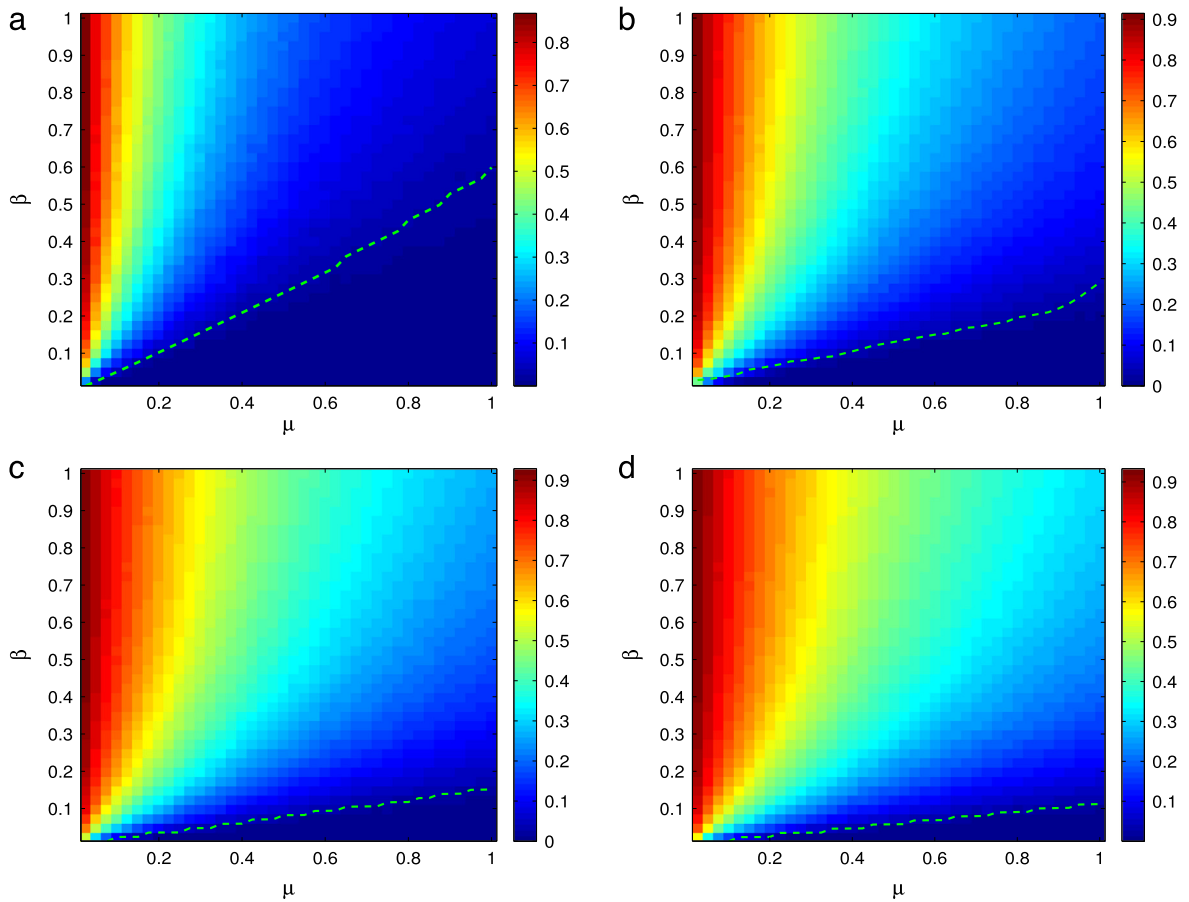


Fig. 3. The comparisons of epidemic thresholds β_c^U using the MMCA approach (green dotted line) and Monte Carlo simulations (heat map) as a function of recovery probability μ . The forgetting probability δ is set as follows: (a) $\delta = 0.2$, (b) $\delta = 0.4$, (c) $\delta = 0.6$, (d) $\delta = 0.8$. The two layers of the multiplex network are the same SF network generated by the configuration model with exponent 3. The Monte Carlo simulations are averaged by 50 realizations. (For interpretation of the references to color in this figure legend, the reader is referred to the web version of this article.)

Table 1
The details of some key parameters.

Parameter	Description
λ	Transition probability from unaware to aware
δ	Transition probability from aware to unaware
β^U	Infection rate for unaware individual
β^A	Infection rate for aware individual
μ	Recovery rate for infected individual
α	The local awareness threshold

corresponds to complete immunity of aware individuals. In order to help the readers have a better understanding of the paper, we summarize the meanings of the parameters for the models in [Table 1](#).

3. Global MMCA method

In the following, with the help of global MMCA method which can be illustrated by the probability tree, we are able to obtain the epidemic threshold of our model [38], as shown in [Fig. 2](#). Actually, the method is the discrete time version of the evolution of epidemics by means of Markov chain. Here, let $\{a_{ij}\}_{N \times N}$, $\{b_{ij}\}_{N \times N}$ be the adjacency matrices of the awareness layer and the contagion layer, respectively. We denote the probabilities of being the three states as $p_i^{AI}(t)$, $p_i^{AS}(t)$, $p_i^{US}(t)$, respectively. And then, on the awareness layer, we define the probability for unaware individual i not changing from state U to state A as $r_i(t)$; on the contagion layer, we define the probabilities for individual i not being infected by any neighbors if i was aware (unaware) as $q_i^A(t)$ ($q_i^U(t)$).

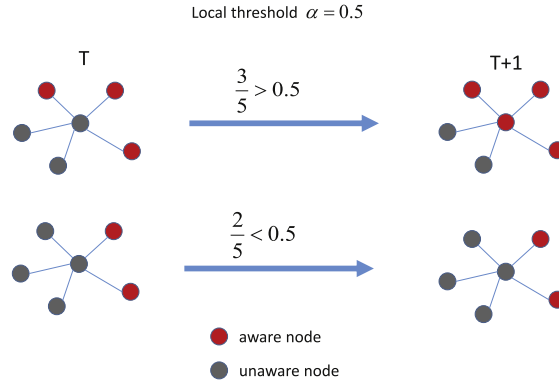


Fig. 4. Illustration of the threshold model used to simulate the spreading of information. Only if the ratio between the number of aware neighbors and its degree is larger than the threshold value α , the unaware individual can become aware. Here, in the toy model, the threshold is set to be 0.5. The red individuals are aware, while the dark ones are unaware. (For interpretation of the references to color in this figure legend, the reader is referred to the web version of this article.)

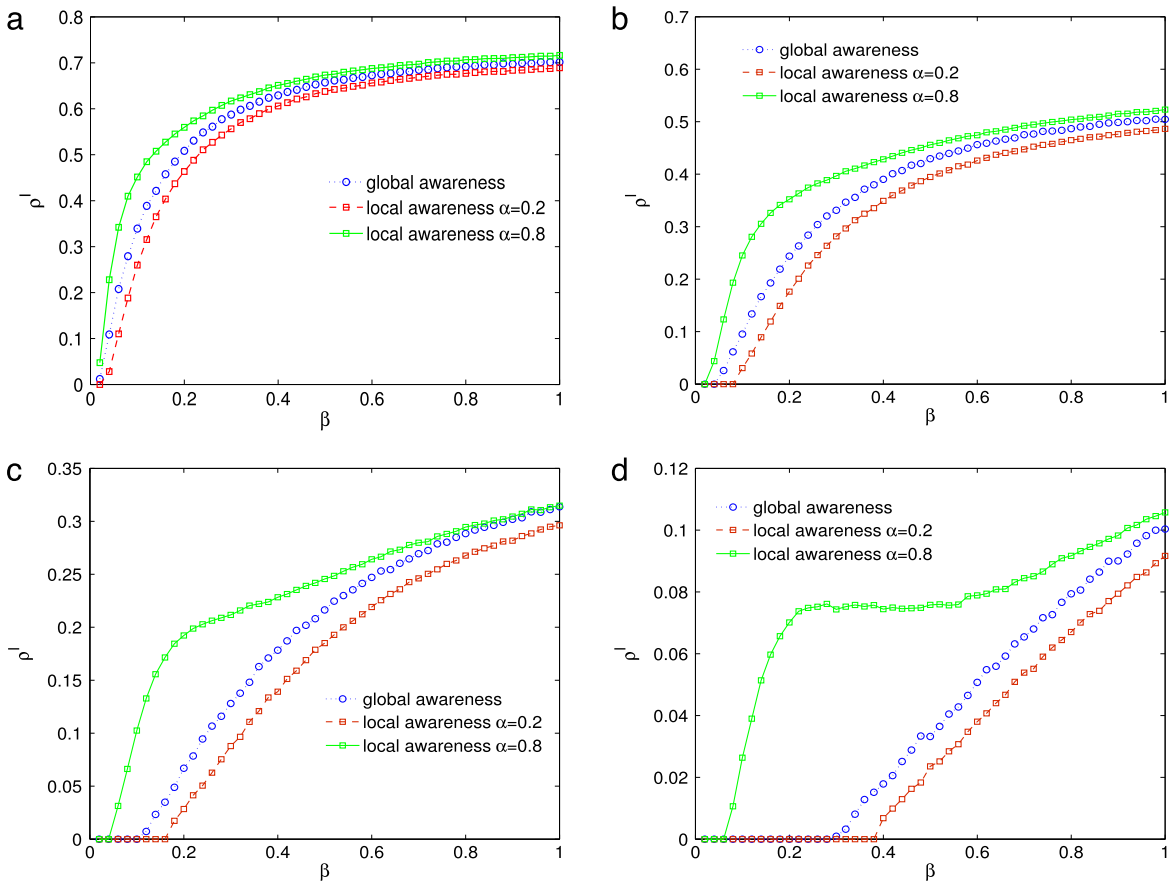


Fig. 5. The comparisons of MC simulations for epidemic spreading between GACS model and LACS model. The multiplex network is the same with the one defined in Fig. 3. The size of infected individuals ρ^i is shown as a function of infectivity β . To be specific, the blue circle dotted lines represent the GACS model, while the green square lines and red square dotted lines correspond to the LACS model with different values of local awareness threshold α . The recovery probability μ and forgetting probability δ are set as follows: (a) $\mu = 0.2$, $\delta = 0.8$, (b) $\mu = 0.4$, $\delta = 0.6$, (c) $\mu = 0.6$, $\delta = 0.4$, (d) $\mu = 0.8$, $\delta = 0.2$. (For interpretation of the references to color in this figure legend, the reader is referred to the web version of this article.)

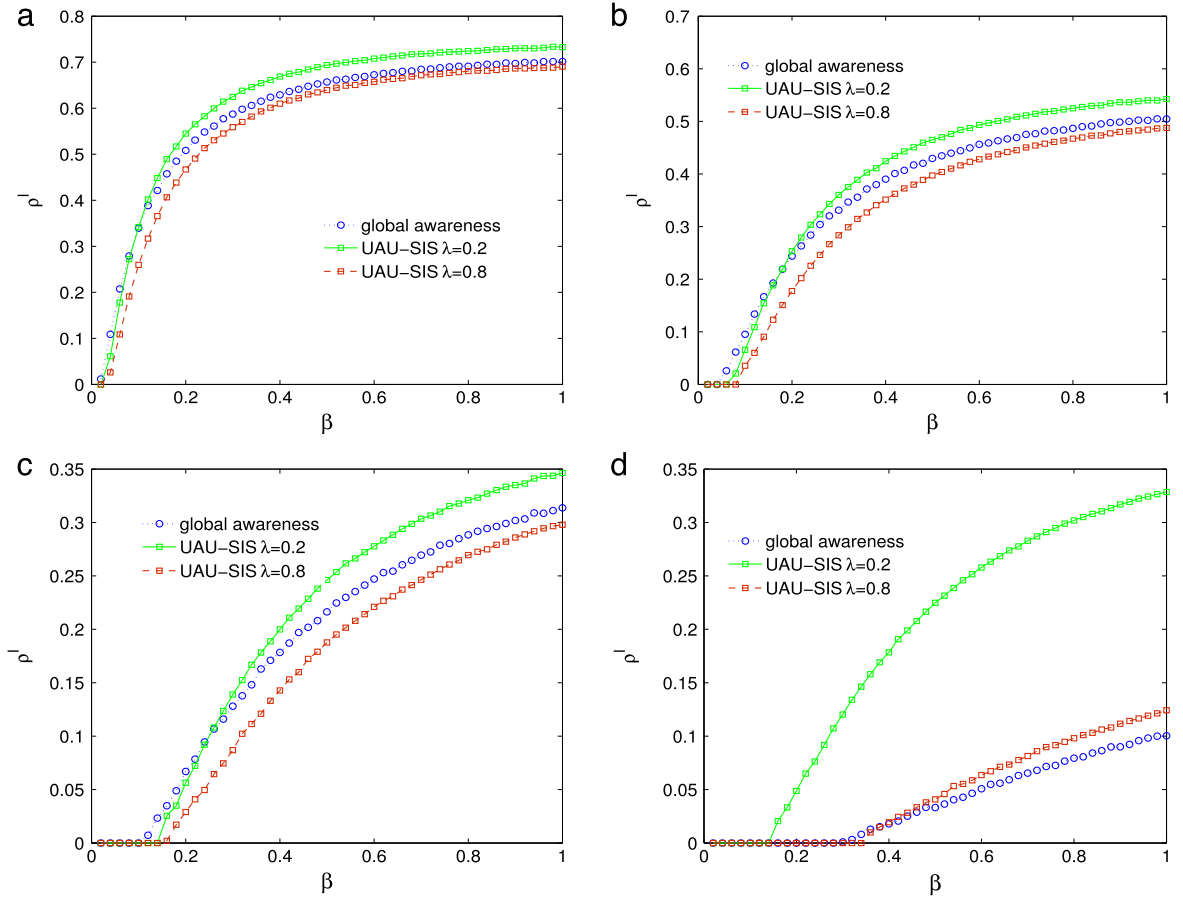


Fig. 6. The comparisons of MC simulations for epidemic spreading between GACS model and SIS–UAU model. The multiplex network is the same with the one defined in Fig. 3. The size of infected individuals ρ^I is shown as a function of infectivity β . The blue circle lines represent the GACS model, while the green square lines ($\lambda = 0.2$) and red square dotted lines ($\lambda = 0.8$) correspond to the SIS–UAU model. The other parameters are set to be: (a) $\mu = 0.2, \delta = 0.8$, (b) $\mu = 0.4, \delta = 0.6$, (c) $\mu = 0.6, \delta = 0.4$, (d) $\mu = 0.8, \delta = 0.2$. (For interpretation of the references to color in this figure legend, the reader is referred to the web version of this article.)

With respect to the above definitions, we have

$$\begin{aligned}
 r_i(t) &= 1 - \frac{\sum_{j=1}^N p_j^A(t)}{N} \\
 q_i^A(t) &= \prod_{j=1}^N (1 - b_{ji} p_j^A(t) \beta^A) \\
 q_i^U(t) &= \prod_{j=1}^N (1 - b_{ji} p_j^U(t) \beta^U).
 \end{aligned} \tag{1}$$

Note that Eqs. (2) are obtained supposing independence on the contribution from the neighbors, which is the only approximation in MMCA [38]. Based on the probability tree and MMCA method, we are able to derive the evolution of each state, just as follows:

$$\begin{aligned}
 p_i^{US}(t+1) &= p_i^{AI}(t) \delta \mu + p_i^{US}(t) r_i(t) q_i^U(t) + p_i^{AS} \delta q_i^U(t) \\
 p_i^{AS}(t+1) &= p_i^{AI}(t) \mu (1 - \delta) + p_i^{US} [1 - r_i(t)] q_i^A(t) + p_i^{AS} (1 - \delta) q_i^A(t) \\
 p_i^{AI}(t+1) &= p_i^{AI}(t) (1 - \mu) + p_i^{US}(t) \{ [1 - r_i(t)] [1 - q_i^A(t)] + r_i(t) [1 - q_i^U(t)] \} \\
 &\quad + p_i^{AS}(t) \{ \delta [1 - q_i^U(t)] + (1 - \delta) [1 - q_i^A(t)] \}.
 \end{aligned} \tag{2}$$

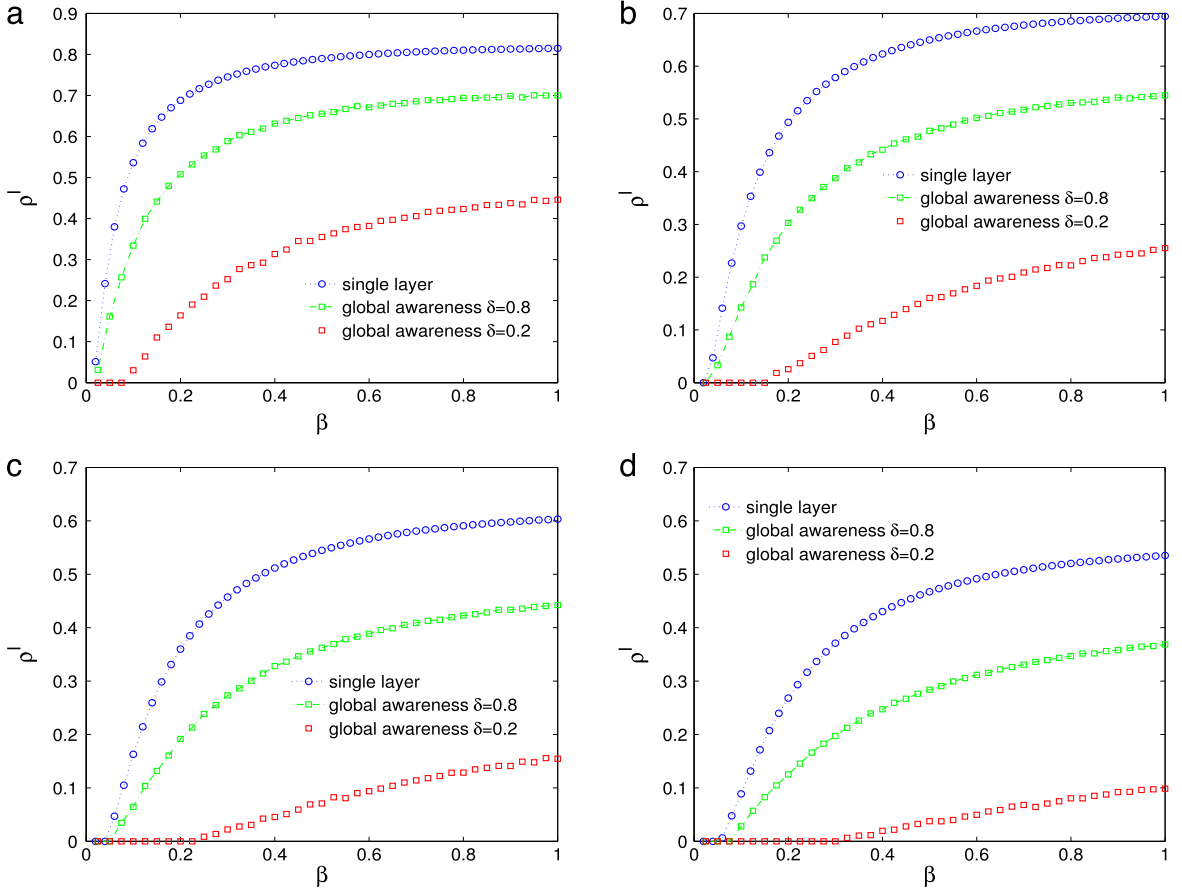


Fig. 7. The comparisons of MC simulations for epidemic spreading between GACS model and single layer occasion. The single layer is just responsible for the epidemic spreading process which is described by the classical SIS model. The multiplex network is the same with the one defined in Fig. 3. The size of infected individuals ρ^i is shown as a function of infectivity β . The blue circle lines represent the single layer occasion, while the green square lines ($\delta = 0.8$) and red square dotted lines ($\delta = 0.2$) correspond to the GACS model. The other parameters are set to be: (a) $\mu = 0.2$, (b) $\mu = 0.4$, (c) $\mu = 0.6$, (d) $\mu = 0.8$. (For interpretation of the references to color in this figure legend, the reader is referred to the web version of this article.)

Since for the epidemic spreading process, there exists a threshold value. It means that only if the infectivity value β is larger than the threshold can epidemic outbreak finally. In order to explore the threshold β_c^U in our model, we need to study the steady state of our model. By letting $t \rightarrow \infty$, which means $\lim_{t \rightarrow \infty} p_i^A(t+1) = p_i^A(t) = p_i^A$, $\lim_{t \rightarrow \infty} p_i^{AS}(t+1) = p_i^{AS}(t) = p_i^{AS}$, we can analyze the critical state of the coupled dynamical processes. Note that around the epidemic threshold β_c^U , the infected probability can be assumed as $p_i^A = \epsilon_i \ll 1$. Besides, we can also simply the probability q_i^A, q_i^U as $q_i^A \approx (1 - \beta^A \sum_j b_{ji} \epsilon_j)$ and $q_i^U \approx (1 - \beta^U \sum_j b_{ji} \epsilon_j)$, respectively. With respect to Eqs. (2) and these approximation, we obtain the reduced stationary equations upon omitting higher-order items:

$$\begin{aligned}
 p_i^{US} &= p_i^{US} r_i + p_i^{AS} \delta \\
 p_i^{AS} &= p_i^{US} (1 - r_i) + p_i^{AS} (1 - \delta) \\
 \mu \epsilon_i &= p_i^{US} ((1 - r_i) \beta^A \sum_j b_{ji} \epsilon_j + r_i \beta^U \sum_j b_{ji} \epsilon_j) + p_i^{AS} (\delta \beta^U \sum_j b_{ji} \epsilon_j + (1 - \delta) \beta^A \sum_j b_{ji} \epsilon_j) \\
 &= (p_i^{AS} \beta^A + p_i^{US} \beta^U) \sum_j b_{ji} \epsilon_j.
 \end{aligned} \tag{3}$$

Noting that $p_i^A + p_i^{AS} + p_i^{US} = 1$, where $p_i^A = p_i^A + p_i^{AS}$. Since $p_i^A = \epsilon_i \ll 1$, we can get $p_i^A \approx p_i^A$ and $p_i^{US} = 1 - p_i^A - p_i^{AS} = 1 - p_i^A$. Therefore, the probability for node i being infected ϵ_i is reduced as follows [38]:

$$\mu \epsilon_i = \beta^U (1 - p_i^A) \sum_j b_{ji} \epsilon_j \tag{4}$$

that is to say, Eq. (4) can also be expressed as

$$\sum_j [(1 - p_i^A) b_{ji} - \frac{\mu}{\beta^U} t_{ji}] \epsilon_j = 0 \tag{5}$$

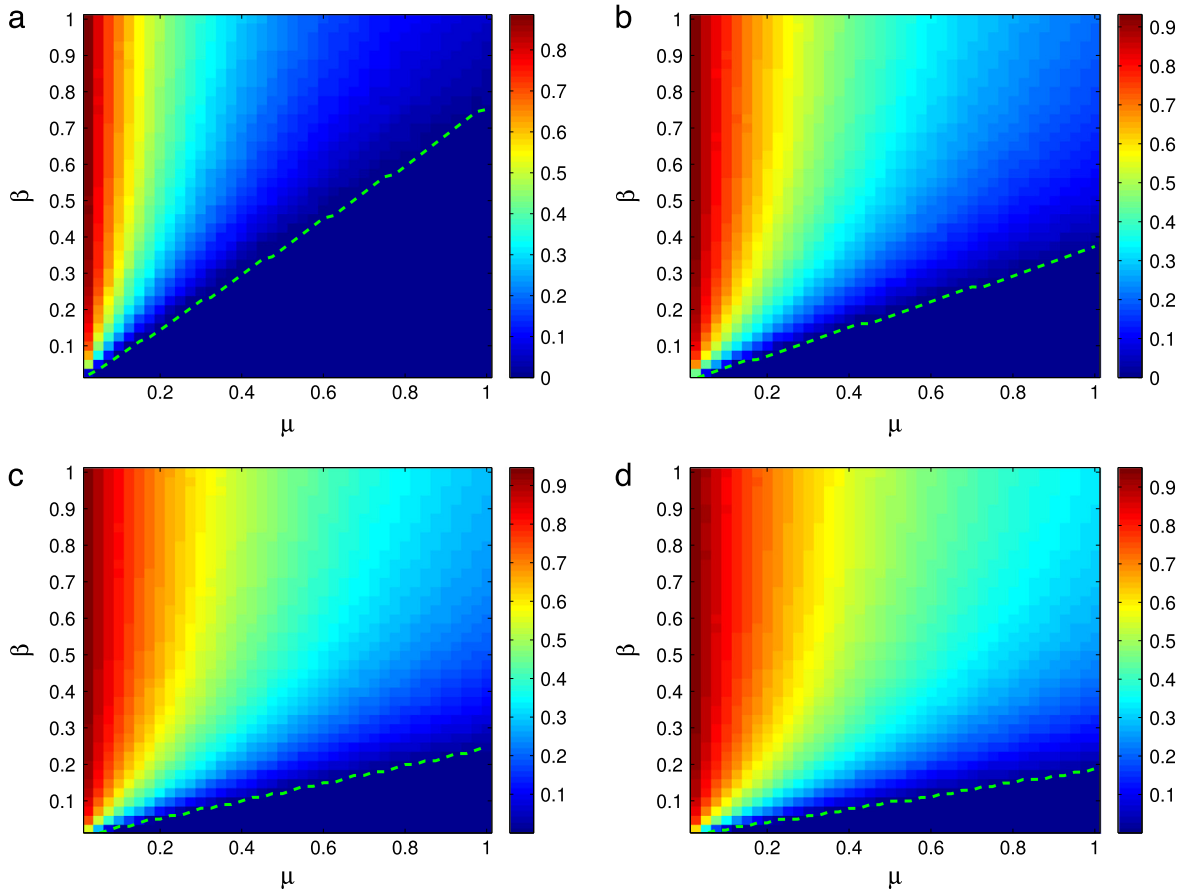


Fig. 8. The comparisons of epidemic thresholds β_c^U using the MMCA approach (green dotted line) and Monte Carlo simulations (heat map) as a function of recovery probability μ . The forgetting probability δ is set as follows: (a) $\delta = 0.2$, (b) $\delta = 0.4$, (c) $\delta = 0.6$, (d) $\delta = 0.8$. The two layers of the multiplex network are the same ER network defined in the main text. The Monte Carlo simulations are averaged by 50 realizations. (For interpretation of the references to color in this figure legend, the reader is referred to the web version of this article.)

where t_{ji} are the elements of the identify matrix. In order to obtain the analytic solution of the epidemic threshold, we introduce a new matrix \mathbf{H} whose elements fulfill $h_{ji} = (1 - p_i^A)b_{ji}$. Then, it is obvious that the epidemic threshold is the one which satisfies

$$\beta_c^U = \frac{\mu}{\Lambda_{max}} \quad (6)$$

where Λ_{max} is the largest eigenvalue of matrix \mathbf{H} .

4. Simulations of the epidemic threshold

After we have the analytic solution of the epidemic threshold β_c^U , it is important for us to crosscheck this with Monte Carlo simulations to see the performance of the global MMCA method. In this section, we use different networks to perform the simulations of the coupled dynamical processes to crosscheck our analytical results. In the following, see Fig. 3, we show the comparisons of Monte Carlo simulations with our theoretical predictions of epidemic threshold β_c^U . The multiplex network consists of two SF networks with 10^4 nodes on each layer, of which the topology structures are the same. Besides, the initial condition is set to be that 10% of nodes are infected. Iterate the rules of the coupled dynamical process with parallel updating until convergence to a steady state. At each time step, all the neighbors of an infected node become infected with the same probability β and the infected node recovers at a rate μ .

It is clear that the MMCA method has a good accuracy to predict the epidemic threshold, no matter what values other parameters are set to be. From the comparison of these figures, we can also find that the forgetting probability δ has obvious effects on the epidemic thresholds. This reflects the importance of considering the awareness spreading during the analysis of epidemic spreading process. Note that in the LACS model, these exist two stage effects resulted by the local awareness threshold, which disappears in the GACS model. In order to explore the difference of epidemic spreading between the GACS

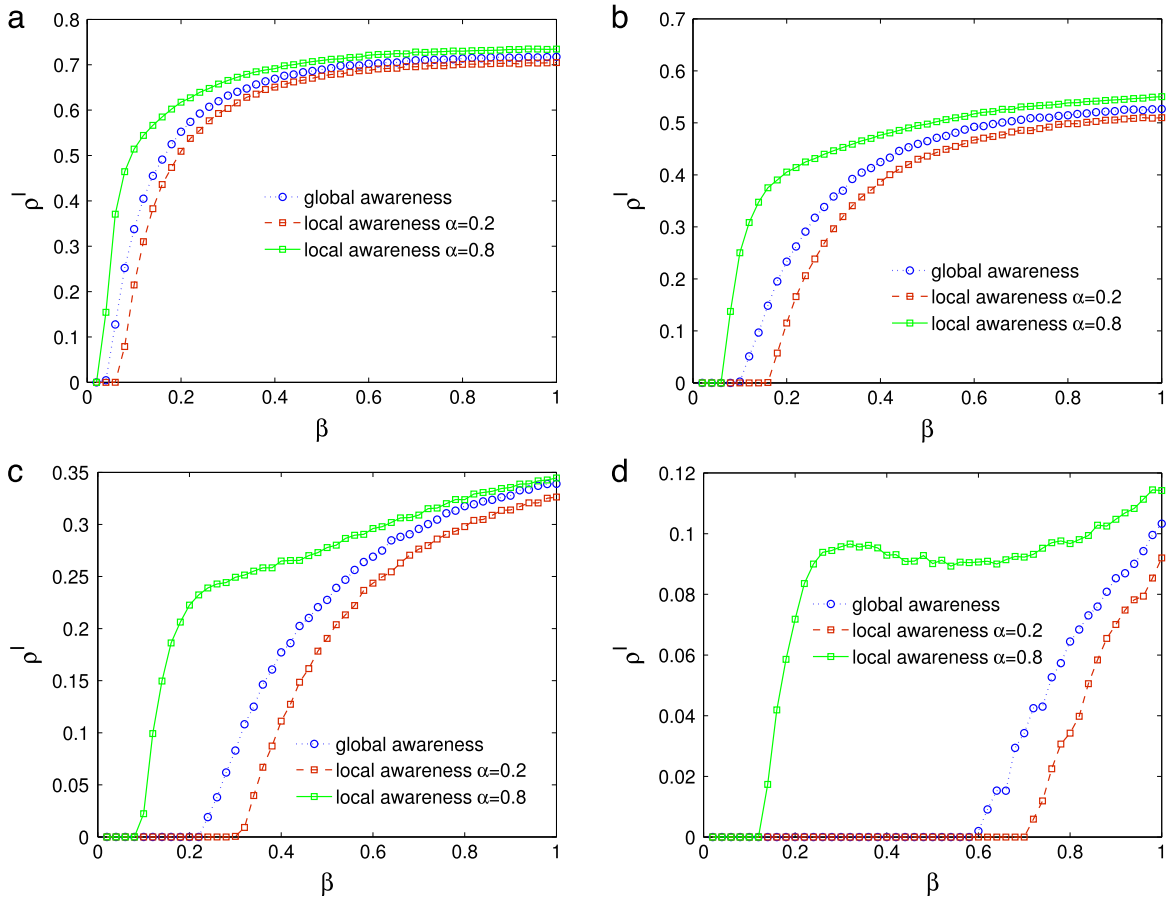


Fig. 9. The comparisons of MC simulations for epidemic spreading between GACS model and LACS model. The multiplex network is a two-layer ER network with 10^4 nodes. The size of infected individuals ρ^I is shown as a function of infectivity β . To be specific, the blue circle dotted lines represent the GACS model, while the green square lines and red square dotted lines correspond to the LACS model with different values of local awareness threshold α . The recovery probability μ and forgetting probability δ are set as follows: (a) $\mu = 0.2, \delta = 0.8$, (b) $\mu = 0.4, \delta = 0.6$, (c) $\mu = 0.6, \delta = 0.4$, (d) $\mu = 0.8, \delta = 0.2$. (For interpretation of the references to color in this figure legend, the reader is referred to the web version of this article.)

model with the LACS model, as well as other classical models, in the following sections, we compare these models under different configurations of parameters.

5. Comparison with local awareness model (LACS)

Since in the LACS model where the upper layer a threshold model as shown in Fig. 4, one of the important parameters is local awareness threshold α and on the two sides of α around 0.5, the epidemic threshold occurs to be quite different [39], in the following, we compare the GACS model with the LACS models under different values of α , as shown in Fig. 5. Some interesting results are revealed in the comparison. Firstly, our simulations crosscheck the two stage effects of the LACS model, because different local awareness thresholds α can result in obvious difference of the coupled dynamical processes. Besides, in the GACS model, the infected percent of individuals ρ^I is larger than that of LACS model with $\alpha = 0.2$, while it is always smaller than that of LACS model with $\alpha = 0.8$. We need to explore the details of the two models to study the discrepancy. As defined in the LACS model, the local awareness threshold α is used to illustrate the probability of the transformation between awareness and unawareness. Lower value of α corresponds to larger probability of being aware for unaware individuals and then it is difficult for the outbreak of epidemics. From the results above, we can find that compared with the LACS model, not only the epidemic threshold, but also the final epidemic size of the GACS model locates between the two categories of the LACS model.

6. Comparison with SIS–UAU model and single layer model

In addition to the LACS models, there still exists a classical coupled spreading model called SIS–UAU, of which the spreading models on the two layers are both actually the SIS model. As for the UAU model, we just need to replace the

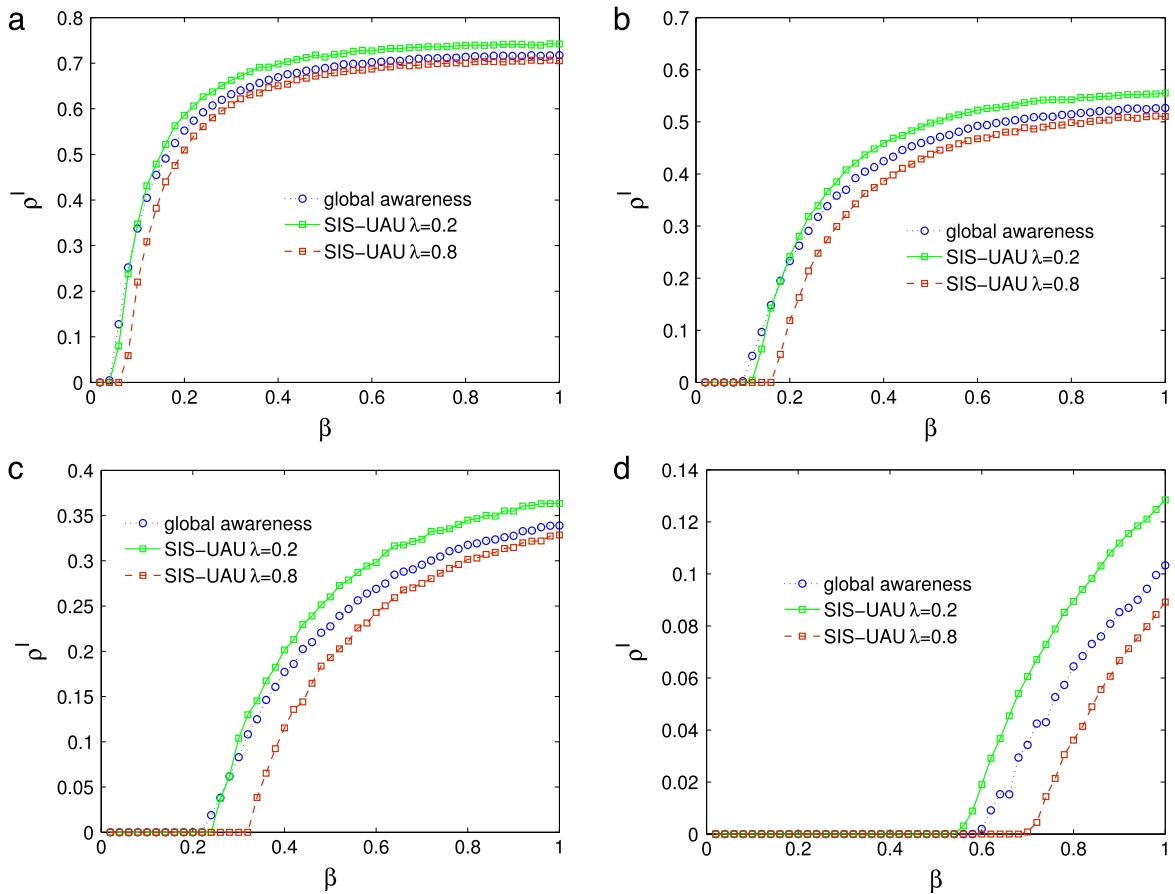


Fig. 10. The comparisons of MC simulations for epidemic spreading between GACS model and SIS-UAU model. The multiplex network is the same with the one defined in Fig. 9. The size of infected individuals ρ^I is shown as a function of infectivity β . The blue circle lines represent the GACS model, while the green square lines ($\lambda = 0.2$) and red square dotted lines ($\lambda = 0.8$) correspond to the SIS-UAU model. The other parameters are set to be: (a) $\mu = 0.2, \delta = 0.8$, (b) $\mu = 0.4, \delta = 0.6$, (c) $\mu = 0.6, \delta = 0.4$, (d) $\mu = 0.8, \delta = 0.2$. (For interpretation of the references to color in this figure legend, the reader is referred to the web version of this article.)

infectivity β and recovery probability μ by aware probability λ and forgetting probability δ , respectively. Hence, compared with the GACS model, a new parameter λ occurs in the SIS-UAU model. According to different values of λ , we compare the GACS model with the SIS-UAU model under the same initial condition.

As illustrated in Fig. 6, on the one hand, for small values of μ and large values of δ , the final epidemic size of GACS model is smaller than that of the SIS-UAU model with small aware probability λ , while it is the larger one if the value of λ is large enough. At the same time, the outbreak of epidemics of the GACS model is always easier than that of other two models, which means that the suppression effects of the GACS model is weaker. On the other hand, for large values of μ and small values of δ , the final epidemic size appears to have the same phenomena, while the opposite occasion occurs about the epidemic threshold. That is to say, the epidemic threshold is not the smallest one. Since μ and δ represent the recovery probability and forgetting probability, respectively, large μ and small δ lead to a larger percent of SA individuals for the GACS model. Hence, it is difficult for the outbreak of epidemics at this condition. Moreover, in order to have a deeper understanding of the global awareness, it is of great importance for us to compare the GACS model with the single layer occasion where no awareness effects exists, as shown in Fig. 7. Taking the forgetting probability δ into consideration, we make comparisons of the two models with different values of δ . As can be seen from the figure, no matter what value μ is, compared with the single layer occasion, the GACS model can lower the final epidemic size and increase the epidemic threshold. In other words, the global awareness is an efficient parameter in the control of epidemics. In addition, we have also performed lots of simulations on Erdős-Rényi (ER) networks and obtained the same results about the GACS model, just as discussed in Appendix section.

7. Conclusion

In a summary, in this paper, through taking the global awareness into consideration, we propose the GACS model to explore the interplay between awareness spreading with epidemic spreading on top of a two-layer multiplex network. The

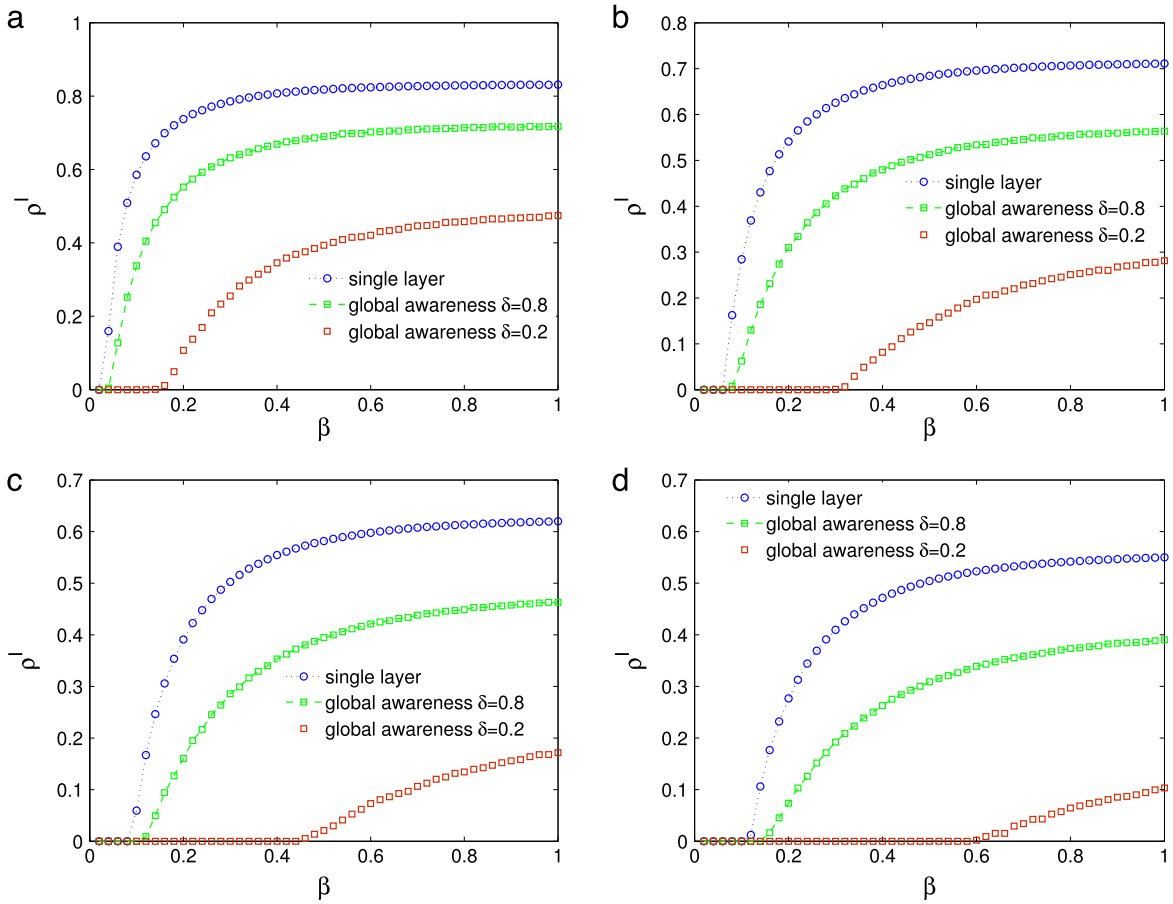


Fig. 11. The comparisons of MC simulations for epidemic spreading between GACS model and single layer occasion. The single layer is just responsible for the epidemic spreading process which is described by the classical SIS model. The multiplex network is the same with the one defined in Fig. 9. The size of infected individuals ρ^I is shown as a function of infectivity β . The blue circle lines represent the single layer occasion, while the green square lines ($\delta = 0.8$) and red square dotted lines ($\delta = 0.2$) correspond to the GACS model. The other parameters are set to be: (a) $\mu = 0.2$, (b) $\mu = 0.4$, (c) $\mu = 0.6$, (d) $\mu = 0.8$. (For interpretation of the references to color in this figure legend, the reader is referred to the web version of this article.)

main difference between the GASC model with other models is that the probability of being aware for unaware individuals is based on the global percent of aware individual in the whole population. Afterwards, we build the probability tree for the coupled dynamical processes to reveal the transitions among different states of individuals. With the help of the global MMCA method, the epidemic threshold can be obtained by solving an eigenvalue problem. Through comparing with lots of Monte Carlo simulations, the method shows high accuracy in predicting the epidemic threshold. Besides, we have also compared the GACS model with some other classical models, including UAU–SIS model, LACS model and single layer occasion, the results reveal abundant details about the differences between different models. Specifically, in the GACS model, there is no two-stage effect which always exists in the LACS model. And if the local awareness threshold α is small enough, the suppression effects of the GACS is weaker than that of the LACS model; while if α is large enough, the suppression effects of the GACS is the stronger one. As for the SIS–UAU model, the epidemic threshold of the GACS model is always smaller, if the value of μ is not so large and δ is not so small. But the final epidemic size depends on the value of λ , for large value of λ , the final epidemic size of the GACS model is the larger one, otherwise, it is the smaller one. Additionally, by comparing with the single layer occasion, it is clear that the GACS model can not only increase the epidemic threshold but also lower the final epidemic size. Our results give us a better understanding of the effects of global awareness and show the importance of taking the information spreading process into account when we try to control the spread of epidemics.

Acknowledgment

This work is partially supported by the Chinese National Science Foundation (NSFC) under Grants No. 61402206 and No. 61672270.

Appendix

In this section, we compare the MMCA method with Monte Carlo simulations on ER networks, just as shown in Fig. 8. Besides, we also compare the GACS model with other classical models which are used to describe the coupled dynamical processes on ER networks. The multiplex network is made up of two ER network with 10^4 nodes on each layer. As illustrated in Figs. 9–11, the LACS model, SIS–UAU model and single layer occasion are all studied in this section through a fully comparison with the GACS model. The figures show the same results with that of SF network. In other words, the results are resulted in by our GACS model itself.

References

- [1] A.L. Barabási, R. Albert, *Science* 286 (5439) (1999) 509–512.
- [2] R. Albert, A.L. Barabási, *Rev. Modern Phys.* 74 (1) (2002) 47.
- [3] M.E.J. Newman, *Phys. Rev. E* 66 (1) (2002) 016128.
- [4] H.E. Stanley, *Introduction To Phase Transitions and Critical Phenomena*, Oxford University Press, Oxford, 1987.
- [5] M. Barthélemy, A. Barrat, R. Pastor-Satorras, A. Vespignani, *Phys. Rev. Lett.* 92 (2004) 178701.
- [6] J. Gómez-Gardeñes, V. Latora, Y. Moreno, E. Profumo, *Proc. Natl. Acad. Sci. USA* 105 (2008) 1399.
- [7] S. Boccaletti, V. Latora, Y. Moreno, M. Chavez, D.U. Hwang, *Phys. Rep.* 424 (4) (2006) 175–308.
- [8] S.V. Buldyrev, R. Parshani, G. Paul, H.E. Stanley, S. Havlin, *Nature* 464 (7291) (2010) 1025–1028.
- [9] A. Arenas, A. Díaz-Guilera, J. Kurths, Y. Moreno, C. Zhou, *Phys. Rep.* 469 (3) (2008) 93–153.
- [10] W. Chen, R.M. D'Souza, *Phys. Rev. Lett.* 106 (11) (2011) 115701.
- [11] D.J. Watts, *Proc. Natl. Acad. Sci. USA* 99 (9) (2002) 5766–5771.
- [12] S. Gomez, A. Diaz-Guilera, J. Gómez-Gardeñes, C.J. Perez-Vicente, Y. Moreno, A. Arenas, *Phys. Rev. Lett.* 110 (2) (2013) 028701.
- [13] J.Q. Kan, H.F. Zhang, *Commun. Nonlinear Sci. Numer. Simul.* 44 (2017) 193–203.
- [14] R. Pastor-Satorras, C. Castellano, P. Van Mieghem, *Rev. Modern Phys.* 87 (3) (2015) 925.
- [15] A. Grabowski, R.A. Kosiński, *Phys. Rev. E* 70 (3) (2004) 031908.
- [16] M.J. Keeling, K.T.D. Eames, *J. R. Soc. Interface* 2 (4) (2005) 295–307.
- [17] S. Funk, M. Salathé, V.A.A. Jansen, *J. R. Soc. Interface* (2010) rsif20100142.
- [18] E. Cozzo, R.A. Banos, S. Meloni, Y. Moreno, *Phys. Rev. E* 88 (5) (2013) 050801.
- [19] M. Kitsak, L.K. Gallos, S. Havlin, F. Liljeros, L. Muchnik, H.E. Stanley, H.A. Makse, *Nat. Phys.* 6 (11) (2010) 888–893.
- [20] M. Salathé, M. Kazandjeva, J.W. Lee, P. Levis, M.W. Feldman, J.H. Jones, *Proc. Natl. Acad. Sci. USA* 107 (51) (2010) 22020–22025.
- [21] V.E. Vergu, H. Busson, P. Ezanno, *PLoS One* 5 (2) (2010) e9371.
- [22] Q.H. Liu, W. Wang, M. Tang, H.F. Zhang, *Sci. Rep.* 6 (2016).
- [23] A. Vespignani, *Nat. Phys.* 8 (1) (2012) 32–39.
- [24] Z. Wang, M.A. Andrews, Z.X. Wu, L. Wang, C.T. Bauch, *Phys. Life Rev.* 15 (2015) 1–29.
- [25] P.J. Mucha, T. Richardson, K. Macon, M.A. Porter, J.-P. Onnela, *Science* 328 (2010) 876.
- [26] M. Szell, R. Lambiotte, S. Thurner, *Proc. Natl. Acad. Sci. USA* 107 (2010) 13636.
- [27] Z. Wang, L. Wang, M. Perc, *Phys. Rev. E* 89 (2014) 052813.
- [28] S. Boccaletti, G. Bianconi, R. Criado, C.I. del Genio, J. Gómez-Gardeñes, M. Romance, I. Sendiña Nadal, Z. Wang, M. Zanin, *Phys. Rep.* 544 (2014) 1.
- [29] M. Kivelä, A. Arenas, M. Barthélemy, J.P. Gleeson, Y. Moreno, M.A. Porter, *J. Comput. Netw.* 2 (3) (2014) 203.
- [30] M. De Domenico, C. Granell, M.A. Porter, A. Arenas, *Nat. Phys.* (2016).
- [31] C. Granell, S. Gómez, A. Arenas, *Phys. Rev. E* 90 (2014) 012808.
- [32] S. Gómez, A. Arenas, J. Borge-Holthoefer, S. Meloni, Y. Moreno, *Europhys. Lett.* 89 (2010) 38009.
- [33] Z. Wang, H. Zhang, Z. Wang, *Chaos* 61 (2014) 1.
- [34] N. Perra, D. Balcan, B. Goncalves, A. Vespignani, *PLoS One* 6 (2011) e23084.
- [35] W. Li, S. Tang, W. Fang, Q. Guo, X. Zhang, Z. Zheng, *Phys. Rev. E* 92 (4) (2015) 042810.
- [36] Q. Guo, Y. Lei, X. Jiang, Y. Ma, G. Huo, Z. Zheng, *Chaos* 26 (2016) 4.
- [37] Q. Guo, Y. Lei, C. Xia, L. Guo, X. Jiang, Z. Zheng, *PLoS One* 11 (2016) e0161037.
- [38] C. Granell, S. Gómez, A. Arenas, *Phys. Rev. Lett.* 111 (2013) 128701.
- [39] Q. Guo, X. Jiang, Y. Lei, M. Li, Y. Ma, Z. Zheng, *Phys. Rev. E* 91 (2015) 012822.
- [40] W. Wang, Q.H. Liu, S.M. Cai, M. Tang, L.A. Braunstein, H.E. Stanley, *Sci. Rep.* (2016) 6.
- [41] C.Y. Xia, S. Meloni, M. Perc, Y. Moreno, *Europhys. Lett.* 109 (5) (2015) 58002.
- [42] H.F. Zhang, J.R. Xie, M. Tang, Y.C. Lai, *Chaos* 24 (4) (2014) 043106.